Journal of Power Sources, 41 (1993) 321–333

The analysis of voltage fluctuations for the characterization of rechargeable alkaline manganese dioxide–zinc cells

P. R. Roberge and M. Farahani
Department of Chemistry & Chemical Engineering, Royal Military College of Canada, Kingston, Ont., K7K 5L0 (Canada)

K. Tomantschger
Battery Technologies Inc., 2480 Dunwin Drive, Mississauga, Ont., L5L 1J9 (Canada)

(Received August 11, 1992; in revised form October 27, 1992)

Abstract

Selected rechargeable 'bobbin-type' alkaline manganese dioxide (RAM)–zinc 'AA' cells were investigated. The cells had an identical design and chemistry with the exception that one group had a conductive coating applied to the inside of the nickel plated steel can which serves as the positive current collector. The electrochemical characterization of the cells was made with various techniques throughout their cycle life. The internal resistance at 1 kHz and electrochemical impedance spectroscopy (EIS) measurements were made at regular intervals on fully charged cells. The voltage fluctuations of the baseline discharge voltage were also recorded during discharge at three moments of the cells' cycle life. These voltage fluctuations were analyzed with a novel analysis technique which relies on the stochastic nature of the voltage fluctuations. The test performed revealed that the can coating contributed to an increase of the overall cell performance. Cells with a coated can exhibited a lower internal resistance and maintained this characteristic even after extended periods of storage.

Introduction

The study of chemical oscillations and electrochemical fluctuations has always fascinated scientists. The early work published in the field of fluctuating electrochemical systems was reviewed in 1972 by Tyagai [1], in 1987 by Bezegh and Janata [2] and in 1988 by Searson and Dawson [3]. Most of the electrochemical noise work published to date has focused on phenomena associated with corrosion studies. Only a limited research effort has been reported [4–10] on the study of the voltage fluctuations associated with the operation of battery systems.

The usefulness of monitoring voltage noise patterns observed during the various phases of charging sealed lead/acid cells was demonstrated [9] by associating the origin of noise signals to problems associated with either the operation of the positive electrode during the earlier phases of charging the cells or the behavior of the negative electrode toward the end of charging. It was also demonstrated [10] that the baseline noise recorded during the simple resistive discharge of Li/SO_2 and $Li/SOCl_2$ cells was related to fundamental characteristics such as cell type and depth-of-discharge.

0378-7753/93/$6.00

But in order to apply noise monitoring in practical production or testing environments as a quality control tool, it became important to transform the information visibly present in the recorded noise spectra into quantitative variables that could eventually become control parameters. An extensive body of literature exists on the various ways of doing such transformations [11, 12], but they have in common a lack of simplicity and appropriateness in the present context since the noise patterns of interest were found to occupy only a relatively narrow frequency domain (1 mHz to 100 Hz).

Stochastic pattern noise analysis

The most common way to analyze noise data has been to transform time records in the frequency domain in order to obtain power spectra. Since noise signals can be produced by either deterministic or stochastic processes and often consist of a complex combination of these processes, the most universal analytical approach has been to correlate predominant frequencies and deconvolute unwanted signals in an iterative manner using well-established mathematical functions. Spectral density plots would thus be computed utilizing fast Fourier transforms (FFT) or other algorithms such as the maximum entropy method (MEM) [13, 14].

Although these techniques find a very appropriate use for the deconvolution of spectroscopic data sets which often contain millions of data points, they can yield disappointing results when applied to smaller sets of data points. The utilization of approximations as in the MEM technique to circumvent this limitation will itself be affected by the presence of nonstationary phenomena which can greatly complicate the final analysis.

The approach taken here for the analysis of voltage fluctuations consisted of two levels of transformation of the original recordings. At the first level the voltage fluctuations were transformed into individual voltage peaks as basic events. This was accomplished relatively simply by sorting the consecutive voltage fluctuations as a function of the recorded voltage changing slopes. Each directional change of the slope of the recorded voltage was used as a trigger and the resulting inter-event times (peak duration) compiled as a basic event in an histogram-type distribution. The rise time of these singular peaks was also sorted in parallel with this first grid since the rise time (dV/dt) is an important characteristic of electrochemical systems. This first level of transformation of incoming signals, which was accomplished by a few lines of BASIC programming language, can yield drastically simplified results (Figs. 1–4).

The approach taken to perform the second level of transformation was imported from the field of statistics of event series such as practiced in reliability engineering [15]. Situations in which discrete events occur randomly in a continuum (e.g. time) and which are called stochastic point processes can normally be described by a Poisson probability distribution $p(x; \lambda t)$, as in eqn. (1), where x represents a random variable, t the specific time involved and λ the mean number of events per unit time:

$$p(x; \lambda t) = \frac{(\lambda t)^x}{x!} e^{(-\lambda t)} \qquad x = 0, 1, 2, \ldots \tag{1}$$

For situations where the hazard rate is constant ($x = 0$), the Poisson probability distribution can be reduced [16] to an exponential distribution (eqn. (2)) where the characteristic parameter (λ) can be easily obtained by integrating the occurrence distribution of the phenomena that have occurred in a given sample:

$$f(t) = \lambda e^{(-\lambda t)} \tag{2}$$

The voltage fluctuations were firstly sorted into peak population distributions which were plotted as cumulative distributions (eqn. (3)) for the evaluation of their

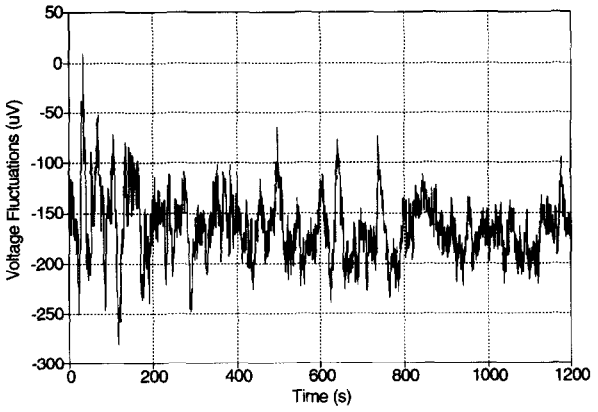

Fig. 1. Example of voltage fluctuations observed during the first 20 minutes discharge of an uncoated can RAM cell.

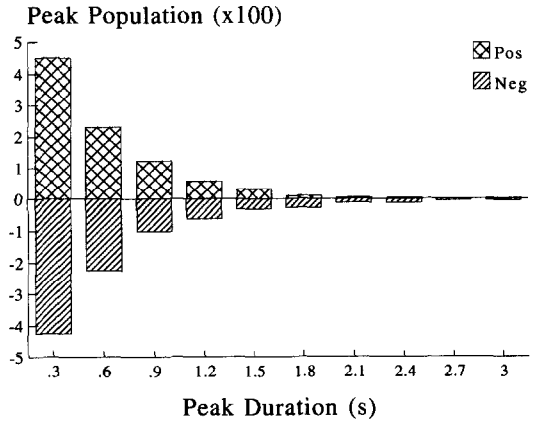

Fig. 2. Voltage fluctuations of Fig. 1 transformed into an histogram of peak population vs. peak duration.

mean number of occurrence:

$$F(t)=\sum \frac{Histogram(t)}{\sum Histogram(t)} \tag{3}$$

The characteristic parameter λ was evaluated at a point of the cumulative distribution given by eqn. (4) which corresponds to a computerized version of the classical method to find λ by plotting data on exponential distribution probability papers:

$$\sum_{t=1}^{1/\lambda} \frac{Histogram(t)}{\sum Histogram(t)} = 0.6321 \tag{4}$$

The goodness-of-fit (GF) of each noise data file was evaluated by comparing the calculated exponential distributions (λ) to the experimental distributions observed.

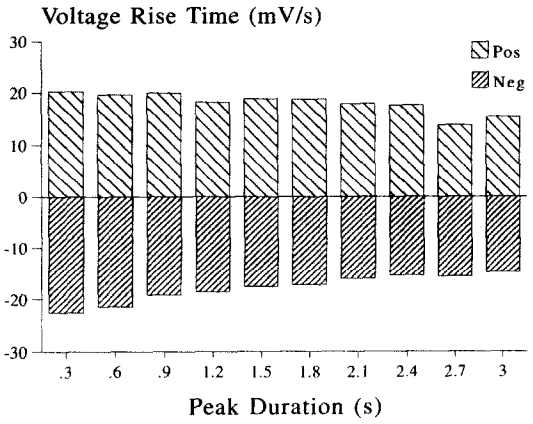

Fig. 3. Average voltage rise time of the fluctuations presented in Fig. 1 as a function of peak duration.

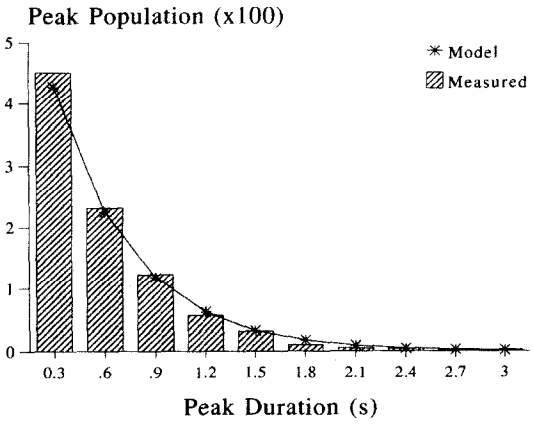

Fig. 4. Distribution of the positive peak duration of Fig. 1 (histogram) and results calculated with the exponential model (curve).

Rechargeable alkaline manganese (RAM) dioxide–zinc technology

In the early 1950s the rechargeability of the MnO_2–Zn system was recognized [17] and efforts commenced to make the 'throw-away' primary alkaline cell rechargeable [18]. The development work revealed that primary alkaline cells, with some design modifications, could be used for applications requiring a relatively inexpensive cell that could deliver a moderate number of cycles, but the first commercial cells produced at the time were plagued with high internal resistance, low nominal capacity and required electronic means to determine the end of discharge [19, 20]. The inability of those cells to handle any kind of consumer abuse resulted in the withdrawal of the rechargeable cells from the market in the early 1970s. The research effort was pursued and new cell designs appeared in the early 1980s [21, 22]. In 1987 the technology was transferred to the Battery Technologies Inc. (BTI) laboratories where the commercial development was intensified.

In the cylindrical cell consumer market RAM cells have become an economically and viable alternative to single use zinc–carbon and alkaline batteries. Most cell components and raw materials used are identical to those used in primary alkaline cells. The major design changes made to primary alkaline cells lie in cathode and anode formulations, the limitation of the anode capacity to less than the first electron capacity of the MnO_2 cathode, the addition of barrier layers to the separator and the integration of means to enable moderate cell abuse. Depending on the conditions of utilization, between 7 to 20 times the operating time of primary alkaline cells and 20 to 50 times that of zinc–carbon cells has been achieved. Current 'AA' RAM cells deliver, during their first cycle, in excess of 125% of the International Electrotechnical Commission (IEC) minimum average for primary alkaline cells and in excess of 80% of the performance of the leading primary alkaline cells on the market. The manufacturing cost of RAM cells is within 120% of the cost of alkaline throw-away cells and the mercury content of commercial design RAM cells has been reduced to the level of present alkaline cells (0.025% of cell weight).

Experimental

In order to determine the effects of can coating on the overall performance of 'bobbin-type' RAM cells, 130 cells were assembled at BTI. These cells were identical in design and chemistry (0.3% Hg based on cell weight) with the exception that one group had a commercially-available carbon-based conductive coating applied to the inside of the can prior to the insertion of the positive electrode while no coating was applied to the nickel-plated can of the second group. These test cells were subsequently submitted to various test procedures commonly used to evaluate alkaline MnO_2–Zn cells.

The initial electrical measurements were taken one week after assembly. The short circuit current was determined using a four probe instrument, to eliminate contact problems, by shorting cells for a period of 150 ms. Closed-circuit voltage measurements were made by applying a 3.9 Ω load to the test cells and recording the cell voltage after 150 ms. In the photoflash test, the RAM cells were exposed to the cyclic imposition of a 1.8 Ω load for 15 s followed by a 45 s period of rest. This sequence was repeated until a 0.9 V threshold was reached. These cycling tests were performed at room temperature after storage for various periods at temperatures between 55 and 65 °C.

The voltage fluctuations were recorded during discharge every ten cycles using a digital multimeter (Fluke Model 8840 A) and a high-pass filter to cut off the d.c. voltage in an experimental set-up described elsewhere [10]. The slowly decreasing cell voltage would appear as a negative offset (≈ -175 μV in Fig. 1) directly related to the slope (dV/dt) of the discharging voltage. For this study, the cells were discharged in a deep discharge fashion with a continuous 3.9 Ω load and a cutoff voltage of 0.75 V after which they were recharged in taper chargers at a maximum current of 500 mA and a 1.72 V maximum voltage over a period of 12 h. A sampling interval (Δt) of 0.3 s and the number of consecutive data points (N) of 4000 were chosen since they allowed access to the frequency domain where electrochemical processes are dominant [3]. The frequency domain corresponding to these sampling conditions can be evaluated to be between 1.7 Hz (f_{max}) and 0.8 mHz (f_{min}) with the help of eqns. (5) and (6) [23]:

$$f_{max} = \frac{1}{2\,\Delta t} \tag{5}$$

$$f_{min} = \frac{1}{N\,\Delta t} \tag{6}$$

The internal resistance (R_{ir}) of fully charged cells was measured with a commercial milliohmmeter (HP Model 4328A) and EIS measurements were obtained at every ten cycles on fully charged cells with a commercial frequency response analyzer (FRA) (Solartron Model 1253) equipped with a potentiostat/galvanostat (Solartron Model 1186).

Results and discussion

Figure 5(a) illustrates the effect of high temperature storage on the short-circuit current of the coated and uncoated test cells. It is apparent cells with a can coating have and maintain higher short-circuit currents which is an indication that the internal resistance of the cells is lowered by the application on the can coating. The short-circuit current of fresh coated cells was determined to be 16.3 A, and 13.2 A for the

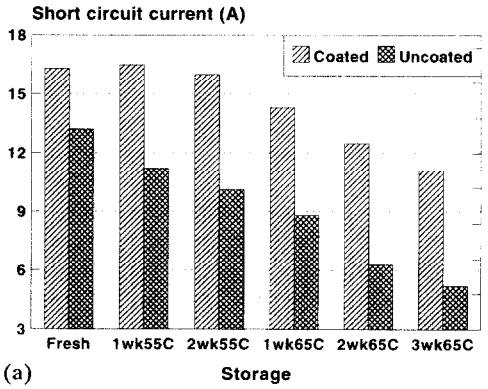

(a)

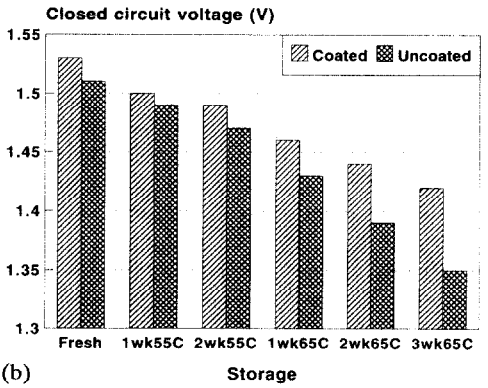

(b)

Fig. 5. (a) Short-circuit current and (b) closed-circuit voltage measured with coated and uncoated RAM cells after storage during various periods at 55 and 65 °C.

uncoated cans. After two weeks storage at 55 °C (equivalent to one year storage at room temperature) the 'AA' RAM cells with the coated can maintained 99% of the original short-circuit current while the uncoated can version could only maintain 79% of their initial short-circuit current. After two weeks at 65 °C (equivalent to 2 years storage at room temperature) the coated can cells still maintained 78% of their initial short-circuit current whereas the uncoated can cells' current dropped to 51% of the initial values. Figure 5(b) contains results describing the behavior of the closed-circuit voltage parameter which was monitored on the two cell designs. Again, the coated can cells outperformed visibly the uncoated can version of these RAM cells.

The performance curves obtained during the 3.9 Ω ambient temperature discharge of RAM cells with coated and uncoated can collectors are presented in Fig. 6(a) with a comparable curve made with a newer technology (1992 design, 0.025% Hg based on cell weight). Figure 6(b) contains performance curves of 1991 cells versus their 1992 counterparts obtained during the photoflash accelerated testing (1.8 Ω). It appears that the motor toy (3.9 Ω) and photoflash (1.8 Ω) performances of the two cell designs to the low voltage cutoffs are very similar. However, a closer analysis of the test data revealed that cells with a can coating exhibited higher average discharge voltages and discharge currents. In the photoflash application this would be translated by more deliverable energy in shorter time periods. As a result, cells with a can coating would have the ability to rejuvenate the flash unit more quickly resulting in the ability to take a sequence of pictures at a much faster rate. It was also noticed that cells with

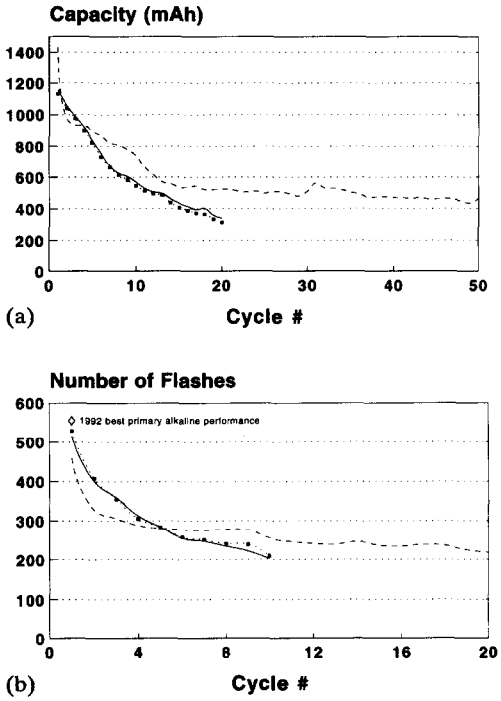

Fig. 6. Average performance of two groups of 1991 (-■-) uncoated and (——) coated can RAM cells deep discharged at (a) 3.9 Ω and (b) 1.8 Ω compared with the performance of (– – –) 1992 RAM cells.

the can coating could deliver more capacity to a higher voltage cutoff than cells without the can coating. This would be a particular asset in applications requiring a constant current discharge and a high voltage cutoff (e.g., 1.1 V).

The analysis of EIS measurements yielded the results presented in Table 1 (uncoated can cells) and Table 2 (coated can cells). This analysis was focused on the EIS data (7 to 1300 Hz) known to be sensitive to the electrochemical interface parameters of interest, i.e., the charge-transfer resistance (R_{ct}) in parallel to the double-layer capacitance (C_{dl}). A third parameter calculated from the EIS data expresses the angle of tilt that is a common feature of EIS Nyquist plots and is apparent in the capacitive range of log(Z) versus log(*Freq*) Bode diagrams [24] as a digression from slope (α) value unity (Figs. 7 and 8). The empirical factor which has to be introduced into the mathematical procedures to fit EIS data would appear as an exponent α with a value between 0 and 1, which would be added to the imaginary component of an impedance frequency (ω) response $Z(\omega)$:

$$Z(\omega) = R_s + \frac{R_{ct}}{1 + (j\omega R_{ct} C_{dl})^{\alpha}} \tag{7}$$

The constant phase element (CPE) corresponding to this empirical factor has often been associated with dispersion effects [25–27] that, in the present case, could be due to a multitude of factors related to the series of interfaces involved between the positive and negative electrodes. The presence and magnitude of the CPE has been demonstrated to be of practical significance for monitoring the health and reliability [28–30] of some chemical power sources (Li/SO_2) that can be modeled with relatively simple equivalent circuits. The magnitude of the CPE ($\propto \omega^{\alpha - 1}$) calculated for the RAM cells tested in the present study can be explained by a broad distribution of values attributed to the activity of the sites involved during the operation of the cells.

TABLE 1

Internal resistance and analyzed EIS results obtained with six uncoated can RAM cells

Cycle no.	R_{ir} (mΩ)	α	R_{ct} (mΩ)	C_{dl} (mF)
2	150 (20)[a]	0.42 (0.05)	170 (20)	1.8 (0.3)
12	260 (20)	0.37 (0.05)	600 (50)	1.0 (0.2)
22	320 (20)	0.36 (0.05)	800 (80)	0.8 (0.2)

[a]Calculated standard deviation.

TABLE 2

Internal resistance and analyzed EIS results obtained with six coated can RAM cells

Cycle no.	R_{ir} (mΩ)	α	R_{ct} (mΩ)	C_{dl} (mF)
2	180 (20)[a]	0.10 (0.08)	240 (20)	1.8 (0.3)
12	270 (20)	0.12 (0.08)	410 (50)	0.9 (0.2)
22	350 (20)	0.14 (0.08)	550 (90)	0.7 (0.2)

[a]Calculated standard deviation.

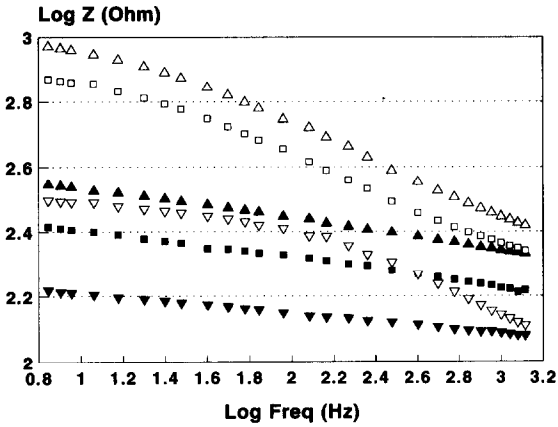

Fig. 7. Bode plots (log(*Z*) vs. log(*Freq*)) of EIS data obtained on fully-charged RAM cells at various points of their cycle life (uncoated can: (▽) cycle no. 2, (□) cycle no. 12, (△) cycle no. 22 and coated can: (▼) cycle no. 2, (■) cycle no. 12, and (▲) cycle no. 22).

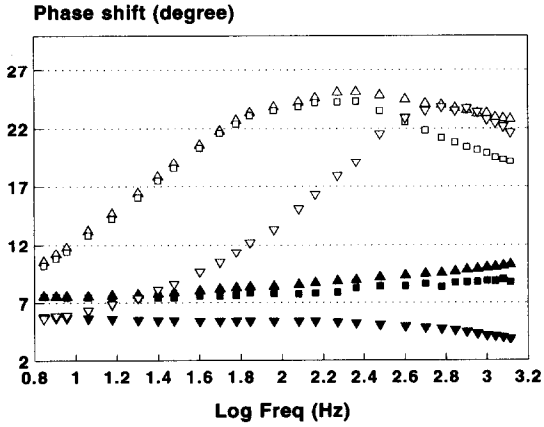

Fig. 8. Bode plots (phase shifts vs. log(*Freq*)) of EIS data obtained on fully-charged RAM cells at various points of their cycle life (uncoated can: (▽) cycle no. 2, (□) cycle no. 12, (△) cycle no. 22 and coated can: (▼) cycle no. 2, (■) cycle no. 12, and (▲) cycle no. 22).

The fact that the CPE apparently increased by adding the conductive coating is probably due to the decreased contribution of the positive electrode to these cells overall impedance (Table 2) thereby increasing the relative importance of the negative electrode. If this is the case, the CPE could partly be attributed to the distributed field caused by the geometry of the negative current collector. But the magnitude of the CPE, which is associated to the dullness of the EIS features (Figs. 7 and 8), also signifies that the RAM cells can not be modeled with simple equivalent circuits thus rendering the interpretation of the differences observed in the parameters calculated from EIS data somewhat uncertain.

The improved conductivity between the positive can collector and the active manganese dioxide became evident during the analysis of the voltage fluctuations

recorded at regular intervals of the cycle life of these cells. The noise analysis was performed with the stochastic pattern detection (SPD) technique presented earlier. The average values of the means (λ) and rise times obtained for the twelve cells tested during this study are presented in Figs. 9 and 10.

The mean values reported in Fig. 9 being an indication of the level of electrochemical noise recorded with the instrumental arrangement used in the present study (sensitivity of filtered voltage ≈ 1 μV), it is quite apparent that the uncoated can cells are much more 'noisy' than their coated counterparts. The level of noise of the uncoated cells also seemed to increase during the cycle life of the RAM cells with the middle of the early cycles (cycle number 3, Figs. 9 and 10) being almost noiseless. A comparison of the voltage rise time of the voltage fluctuations (Fig. 10) calculated with the SPD

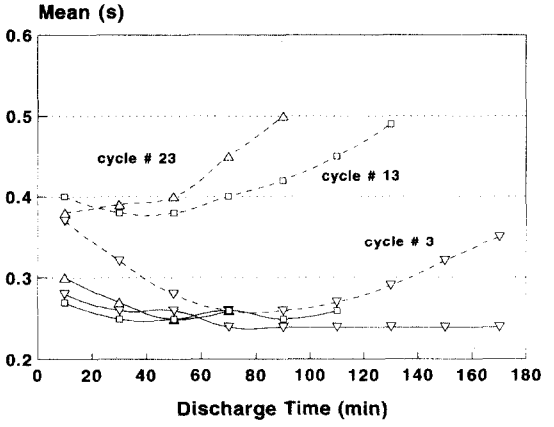

Fig. 9. Average of the means (λ) calculated with the SPD technique of the voltage noise fluctuations recorded during the discharge of (– – –) uncoated and (——) coated can RAM cells ((▽) cycle no. 3, (□) cycle no. 13, and (△) cycle no. 23).

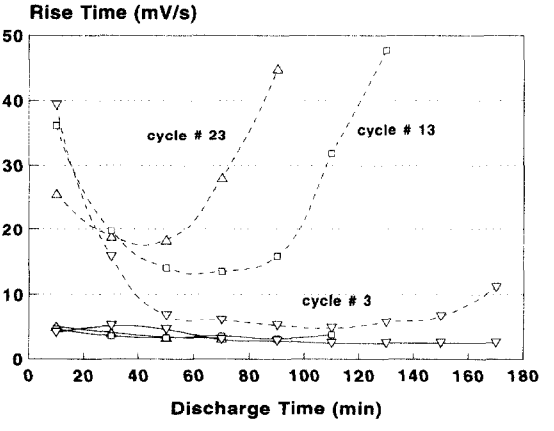

Fig. 10. Average of the rise times measured during the discharge of (– – –) uncoated and (——) coated can RAM cells ((▽) cycle no. 3, (□) cycle no. 13, and (△) cycle no. 23).

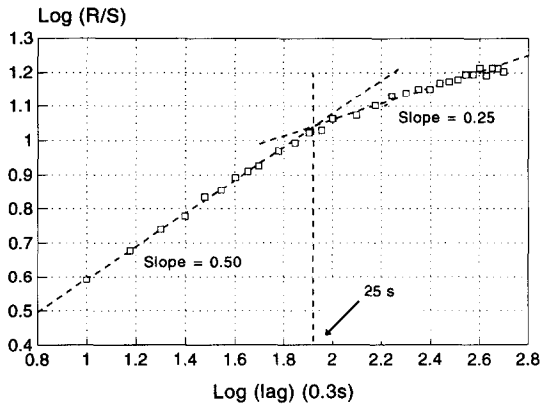

Fig. 11. Rescaled range analysis of the noise sample presented in Fig. 1.

technique also indicated that almost no observable difference existed for the coated RAM cells while the rise time of uncoated can cells dropped to a minimum value part-way through discharge, then increased.

The average goodness-of-fit by the SPD technique of over 80 h of noise measurements made during this study was evaluated to be 97.7%. A similar goodness-of-fit value was obtained when synthetic files of either white of 'brown' (from Brownian motion) noise were tested thus confirming that most of the voltage fluctuations observed with the RAM cells are produced by stochastic processes. This observation was tested against one of the most useful mathematical models for analyzing time-series data which was proposed a few years ago by Mandelbrot and van Ness [31]. Although the fractional Brownian motion (fBm) model can help to describe very complex geometries or time series, its analysis can be made in relatively simply by using the rescaled range analysis or R/S technique, where R or $R(t, s)$ stands for the sequential range of the data points increments for a given lag s and time t and S or $S(t, s)$ for the square root of the sample sequential variance, which was originally proposed by Hurst [32] and applied by Mandelbrot and Wallis [33] to the determination of the fractal characteristics of a time-series [34].

Figure 11 presents the results obtained by transforming the noise sample of Fig. 1 into a R/S or Pox plot. It can be seen that this noise sample seems to be governed by two modes which correspond to two slopes on the Pox plot (Fig. 11). Hurst [32] and later Mandelbrot and Wallis [33] have proposed that the ratio R/S is a random function with scaling properties of dimension H (the slope of a Pox plot). A slope of 0.5 would correspond to a fractal dimension of 1.5 which is itself characteristic of the well-known Brownian motion. A slope differing from 0.5 would be characteristic of what was termed fBm. The initial slope of 0.50 in Fig. 11 would correspond to the predominance of Brownian motion in the frequency range of 1.7 Hz (f_{max}) and 40 mHz (lag = 25 s) and to a different mode (slope 0.25) for lower frequencies. A slope smaller than 0.5 would reveal the presence of anti-persistence [34] and indicate that a negative correlation exists between past and present trends. By experimenting with synthetic noise files it can also be concluded that a slope of 0.2 on a Pox plot corresponds to a typical $1/f$ decay while the Brownian motion decays with a $1/f^2$ ratio.

Conclusions

A total of 130 'AA' RAM test cells were assembled and exposed to a variety of test procedures to determine the effect of applying a carbon-based coating, to the inside of the nickel-plated steel can. The standard electrical tests performed during this study permitted to demonstrate the increase in performance achieved by adding the conductive can coating. Cells with a coated can exhibited overall lower internal resistance and maintained this characteristic even after extended periods of storage at different temperatures. The various tests performed made it obvious that cells utilizing a can coating maintained their electrical performance over their cycle life while cells with an uncoated can deteriorated at a faster rate, particularly in situations requiring a high voltage cutoff or after high temperature storage.

The application of the SPD technique to the analysis of spontaneous electrochemical noise also revealed that the presence of an additional layer of conductive coating between the can collector and the positive material drastically reduced the amplitude of the voltage fluctuations recorded during the discharge of these test cells. The voltage fluctuations recorded in the present study can thus be attributed almost entirely to differences in the electrical contact between the can collector and the active cathode material, the plated nickel having a tendency to passivate and become less conductive with usage. The results of analysis of all the noise samples gathered during this study indicated that the SPD technique fitted almost perfectly the noise signatures generated during the lifetime of the RAM cells. The rescaled range analysis performed on typical noise samples confirmed that the noise signatures were indeed produced by stochastic processes generating Brownian motion signals in the frequency domain of analysis.

EIS and internal resistance measurements were also made during the lifetime of the cells tested. They proved to be relatively insensitive to the two different technologies tested in this study except for the general aspects of the EIS plots which were much more diffuse in the case of cells with a conductive can coating. Additional work is presently being carried out with flat plate RAM cells into which it is possible to add a reference electrode and perform EIS and electrochemical noise (EN) measurements in various three-electrode configurations. It is hoped that the results obtained with this work will permit to develop the models necessary to understand more fully the features revealed in the present study by both EIS and EN measurements.

References

1 V. A. Tyagai, *Elektrokhimiya, 10* (1974) 3.
2 A. Bezegh and J. Janata, *Anal. Chem., 59* (1987) 494A.
3 P. C. Searson and J. L. Dawson, *J. Electrochem. Soc., 135* (1988) 1908.
4 K. F. Knott, *Electron Lett., 1* (1965) 132.
5 A. Chabli, J. P. Diard, P. Landau and B. LeGorrec, *Electrochim. Acta, 29* (1984) 509.
6 C. Gabrielli, F. Huet and M. Keddam, in A. D'Amico and P. Mazetti (eds.), *Noise in Physical Systems and 1/f noise,* Elsevier, Amsterdam, 1986, p. 214.
7 G. Verville, P. R. Roberge and J. Smit, in *Power Sources 12,* Int. Power Sources Symp. Committee, Leatherhead, UK, 1989, pp. 43–60.
8 G. Verville, P. R. Roberge, R. Beaudoin and J. Smit, in *Proc. 9th Int. Electric Vehicle Symp., Toronto, Nov. 13–16, 1988,* EVSS88-060.
9 P. R. Roberge, R. Beaudoin, G. Verville and J. Smit, *J. Power Sources, 27* (1989) 177.
10 P. R. Roberge, E. Halliop and M. D. Farrington, *J. Power Sources, 34* (1991) 233–241.
11 J. S. Bendat and A. G. Piersol (eds.), *Engineering Applications of Correlation and Spectral Analysis,* Wiley-Interscience, New York, 1980.

12 J. S. Bendat and A. G. Piersol (eds.), *Random Data: Analysis and Measurement Procedures,* Wiley-Interscience, New York, 2nd edn., 1986.
13 N. Andersen, *Modern Spectrum Analysis,* Institute of Electric and Electronic Engineers, New York, NY, 1978.
14 N. Andersen, *Geophysics, 39* (1974) 69.
15 P. D. T. O'Connor (ed.), *Practical Reliability Engineering,* Wiley-Interscience, New York, 2nd edn., 1989.
16 R. E. Walpole and R. H. Myers (eds.), *Probability and Statistics for Engineers and Scientists,* MacMillan, London, 4th edn., 1989.
17 H. Y. Kang and C. C. Liang, *Electrochim. Acta, 13* (1968) 277.
18 L. F. Urry, *US Patent 3 024 297* (1962).
19 S. U. Falk, *Batteries—Manganese Dioxide,* Vol. 1, Wiley–Interscience, New York, 1969.
20 D. Linden (ed.), *Handbook of Batteries and Fuel Cells,* McGraw-Hill, New York, 1984.
21 K. Kordesch, *Electrochim. Acta, 25* (1981) 232.
22 K. Kordesch and J. Gsellmann, *US Patent 4 384 029* (1983).
23 J. C. Uruchurtu and J. L. Dawson, *Corrosion, 43* (1987) 19.
24 S. Lin, S. Kim, H. Shih and F. Mansfeld, *Electrochim. Acta, 34* (1989) 1123.
25 K. S. Cole and R. H. Cole, *J. Chem. Phys., 9* (1941) 341.
26 D. W. Davidson and R. H. Cole, *J. Chem. Phys., 19* (1951) 1484.
27 A. K. Jonscher (ed.), *Dielectric Relaxation in Solids,* Chelsea Dielectrics Press, London, 1983.
28 C. D. Jaeger, S. C. Levy, E. V. Thomas and J. T. Cutchen, *J. Power Sources, 20* (1987) 27.
29 C. D. Jaeger, N. H. Hall and E. V. Thomas, *Lithium Ambient-Temperature Battery Reliability Program, SAND87-2119,* Sandia National Laboratories, Albuquerque, NM, 1989.
30 C. D. Jaeger, in *Proc. Symp. Lithium Batteries,* The Electrochemical Society, Princeton, NJ, 1987, p. 93.
31 B. B. Mandelbrot and J. W. van Ness, *SIAM Review, 10* (1968) 422.
32 E. H. Hurst, in *Proc. Inst. Civ. Eng., 5 Part I,* 1956, p. 519.
33 B. B. Mandelbrot and J. R. Wallis, *Water Resources Res., 5* (1969) 321.
34 L. T. Fan, D. Neogi and M. Yashima (eds.), *Elementary Introduction to Spatial and Temporal Fractals,* Springer, Berlin, 1991.